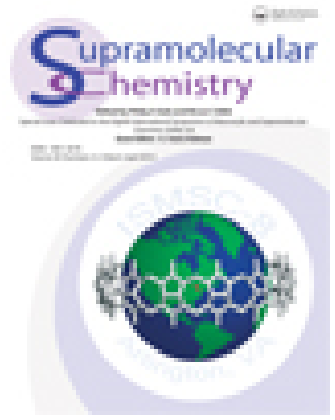

Supramolecular Chemistry
Publication details, including instructions for authors and subscription information:
http://www.tandfonline.com/loi/gsch20

Solid-phase Pd-catalysed cross-coupling methods for the construction of π-conjugated peptide nanomaterials

Allix M. Sanders[a] & John D. Tovar[abc]

[a] Department of Chemistry, Johns Hopkins University, Baltimore, MD 21218, USA

[b] Department of Materials Science and Engineering, Johns Hopkins University, Baltimore, MD 21218, USA

[c] Institute for NanoBiotechnology, Johns Hopkins University, Baltimore, MD 21218, USA

Published online: 22 Nov 2013.

To cite this article: Allix M. Sanders & John D. Tovar (2014) Solid-phase Pd-catalysed cross-coupling methods for the construction of π-conjugated peptide nanomaterials, Supramolecular Chemistry, 26:3-4, 259-266, DOI: 10.1080/10610278.2013.852675

To link to this article: http://dx.doi.org/10.1080/10610278.2013.852675

Supramolecular Chemistry, 2014
Vol. 26, Nos. 3–4, 259–266, http://dx.doi.org/10.1080/10610278.2013.852675

Taylor & Francis
Taylor & Francis Group

Solid-phase Pd-catalysed cross-coupling methods for the construction of π-conjugated peptide nanomaterials

Allix M. Sanders[a] and John D. Tovar[a,b,c]*

[a]*Department of Chemistry, Johns Hopkins University, Baltimore, MD 21218, USA;* [b]*Department of Materials Science and Engineering, Johns Hopkins University, Baltimore, MD 21218, USA;* [c]*Institute for NanoBiotechnology, Johns Hopkins University, Baltimore, MD 21218, USA*

(*Received 16 July 2013; accepted 2 October 2013*)

We describe the development of two procedures for the synthesis of peptides that are embedded with a variety of π-conjugated semi-conducting oligomers. These procedures utilise solid-phase variants of classical palladium-catalysed cross-couplings commonly used to prepare π-conjugated oligomers. The resulting peptide–π–electron hybrids are soluble in aqueous media and self-assemble to produce 1D nanostructures, simultaneously forming networks of π-stacked conduits. The procedures have allowed for the inclusion of complex chromophores including mixed aryl units, ethynylene linkers and sexithiophenes where the latter peptide's nanostructures demonstrated substantial conductivity when employed as an active layer in a field-effect transistor.

Keywords: bioelectronics; supramolecular polymers; organic electronics; self-assembly

1. Introduction

The construction of organic bioelectronic materials based on non-covalent electronic delocalisation is a current challenge for organic materials science (*1–3*). One means to produce these types of materials is by modifying peptides that are able to undergo self-assembly to afford supramolecular electronic nanostructures that are water processable and potentially biologically relevant (*4–11*). For example, peptide backbones with embedded π-conjugated subunits can self-assemble in aqueous environments thereby forming β-sheet-rich supramolecular nanostructures of high aspect ratio that support extended π-stacked conduits. These types of systems are attractive because the peptidic self-assembly allows for facile but precise organisation of electrically conductive units. Furthermore, the peptide scaffolds can be adapted for biological compatibility and can act as a bridge between the biotic and abiotic worlds, with potential applications in electrically controlled cell regeneration or biosensing. However, preparing these types of modified peptides has required lengthy solution-phase synthesis and purification of the π-conjugated units, thus slowing the process of creating diverse libraries of π-conjugated peptides.

Solid-phase syntheses have been used extensively for the rapid construction of a variety of molecules. Instead of requiring time-consuming solution-phase purification after each step of a synthetic route, catalysts, side products and reagents can simply be washed from the polymer support prior to cleaving the product from the resin and isolating it in relatively pure form. This method has been widely used for the synthesis of biological materials such as peptides and oligonucleotides, and has also been adapted to perform a variety of other chemical transformations, such as palladium-catalysed cross-couplings to form new carbon–carbon and carbon–heteroatom bonds (*12–14*). For example, solid-phase Stille and Suzuki cross-couplings have been broadly employed for the creation of potential pharmaceuticals and π-conjugated oligomers (*15–24*). Solid-phase chemistry has also been used for intramolecular macrocycle formation due to the 'pseudo-dilution effect' inherent to resins with low loading concentrations (*25*), but intermolecular site-to-site reactions between molecules adjacent to one another on a resin bead ('cross-linking') are also known on highly loaded resins. Taking advantage of this site–site reactivity allows for the formation of homodimers on the solid phase, and a wide variety of homodimers have been prepared using transition metal coupling procedures such as ring-closing metathesis to produce alkene linkages and various acetylenic homocouplings to produce butadiyne linkers (*26–29*). In this study, we describe the development of two on-resin Pd-catalysed methods that lead to self-assembling peptide–π–peptide triblock molecules, one previously unpublished, and one recently communicated (*30*).

*Corresponding author. Email: tovar@jhu.edu

2. Results and discussion

2.1 Synthetic approaches for π-conjugated peptides

Our group previously harnessed site–site reactivity whereby reactive π-conjugated bis-electrophiles led to diimidation/diamidation cross-linking of resin-bound peptides to produce modified peptide–π–peptide triblock molecules (*31*). However, we found that longer oligomers to be used for cross-linking were synthetically difficult to achieve and insufficiently soluble in synthetic solvents. To further exploit the facile nature of solid-phase synthesis for the preparation of aqueous self-assembling π-conjugated peptides, we envisioned the creation of methods that employ solid-phase palladium-catalysed cross-couplings (Stille, Suzuki and Sonogashira) in conjunction with standard solid-phase peptide synthesis (SPPS). In contrast to solution-phase syntheses, these methods would allow for the rapid synthesis of a variety of π-conjugated peptides from commercially available or readily synthesised small molecule components, without the need for prior molecular synthesis of the entire π-conjugated cross-linking agent.

We developed two methods as outlined in Figure 1. In both cases, Fmoc-based SPPS is performed to synthesise oligopeptides bound to a resin bead. An aryl group (Ar^1) substituted with a carboxylic acid and a halide is then introduced to the resin under standard activation conditions for peptide amidation (O-(Benzotriazol-1-yl)-*N,N,N′,N′*-tetramethyluronium Hexafluorophosphate (HBTU), Diisopropylethylamine). Amidation occurs between the carboxylic acid groups of the arenes and the deprotected amine termini of the resin-bound peptide chains leading to the common peptide resin shown in Figure 1. In procedure 1, another arene (Ar^2) that is substituted with functionality necessary for cross-coupling under palladium catalysis (e.g. a tributyl stannane group) and also functionalised with an Fmoc-protected amine is introduced to the resin. In the presence of a palladium catalyst, cross-coupling between the Ar^2 and the Ar^1-terminated peptide fragments occurs. The resulting Fmoc-protected aryl-capped peptides can be deprotected by treating the resin with a 20% piperidine solution just like a normal Fmoc-protected amino acid, and SPPS can be continued. After cleaving from the resin, the desired peptide embedded with an $Ar^1–Ar^2$ moiety is obtained. In procedure 2, an arene (Ar^2) that is disubstituted with substituents for cross-coupling is introduced to the Ar^1-capped resin in the presence of a palladium catalyst. Double cross-coupling occurs between Ar^2 and two peptides near to one another on a resin bead presenting the Ar^1 termini to give the locally cross-linked structure. Treating the resin with standard peptide cleavage conditions affords the desired peptide with an extended $Ar^1–Ar^2–Ar^1$ π-conjugated moiety embedded in the peptide backbone.

A peptide synthesised as a test case via procedure 1 is shown in Figure 2. Following SPPS, 2-bromothiophene carboxylic acid was coupled to the amine termini of the peptide chains via amidations under HBTU activation conditions. Stille cross-coupling conditions were used to couple the resin-bound 2-bromothiophene carboxamide moiety with stannylated Fmoc-protected thiophene amine to give a resin-bound peptide bearing a terminal bithiophene. This unit was then treated under standard SPPS to continue peptide growth, and subsequent cleavage from the resin afforded compound **1**. In principle, we could use more complex Ar^2 units, but in practice, their synthesis with the requisite Fmoc groups was quite difficult, requiring multiple steps due to the asymmetry of the molecule, as well as multiple protecting group interconversions due to the sensitivity of the Fmoc-protecting group to *n*-butyllithium, which is necessary for stannylation (*32*). This method also requires additional SPPS in

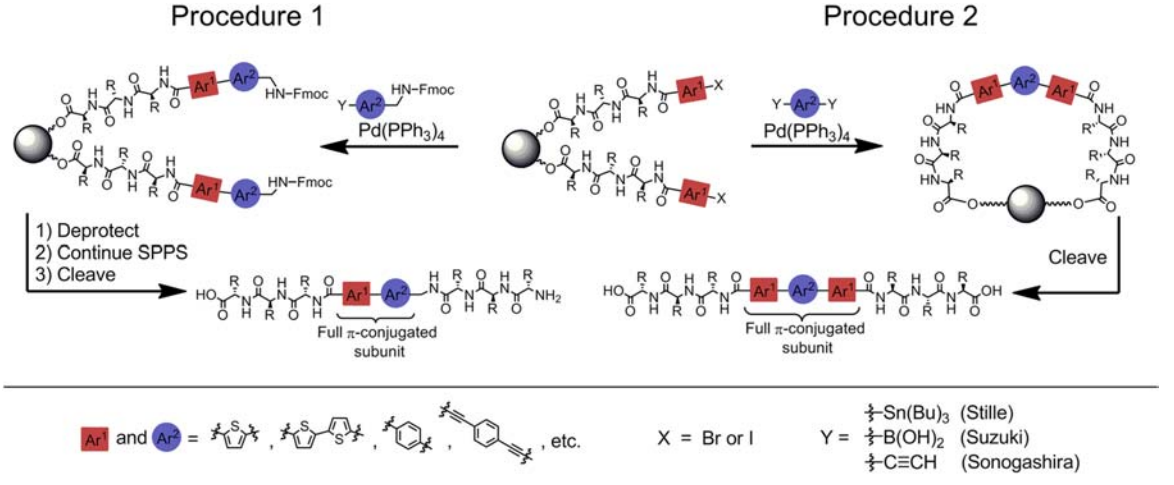

Figure 1. (Colour online) Solid-phase Pd-catalysed cross-coupling procedures.

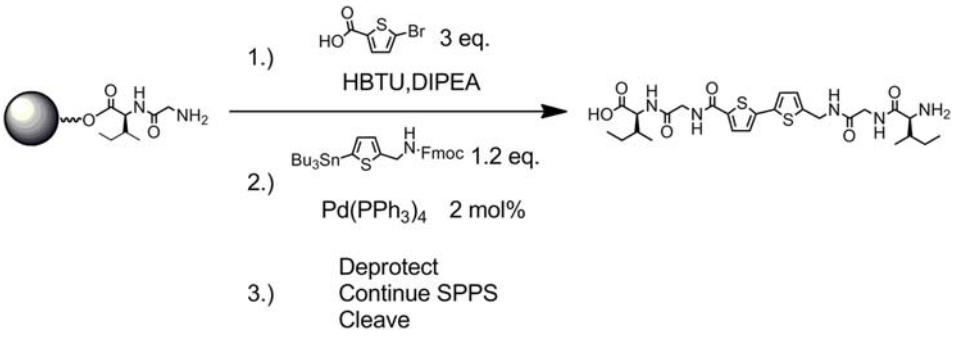

Figure 2. Peptide prepared from procedure 1.

order to extend the peptide backbone. While this allows for the variation in primary amino acid sequence on either side of the chromophore, difficulties in Ar^2-Fmoc preparation led us to pursue an alternative strategy.

We sought a new strategy that capitalised on the ease of the on-resin dimerisation cross-linking and on the versatility of Pd-mediated cross-coupling. This led to the development of procedure 2, enabling access to a variety of peptides summarised in Figure 3 (*30*). After completion of the peptide synthesis via SPPS, diverse *N*-acyl end caps consisting of thiophene, bithiophene and phenyl arenes (Ar^1) were coupled to the resin via standard HBTU-mediated amidation. The resin was then treated with a doubly reactive second arene (Ar^2) under various palladium-catalysed cross-coupling conditions. Utilising Stille cross-coupling conditions with thiophene and bithiophene-based end-capped peptides and disubstituted transmetallating agents, peptides embedded with oligothiophene chromophores of varying length were synthesised from terthiophene (**2**) to sexithiophene (**5**). 4-Iodophenyl carboxamide-capped peptides were subjected to Suzuki conditions in the presence of 1,4-benzene diboronic acid and Sonogashira conditions with 1,4-diethynyl benzene to give oligophenylene-containing **6** and oligophenyleneethynylene-containing **7**, respectively. In addition, Stille or Suzuki conditions were used to give peptides embedded with chromophores consisting of alternating patterns of thiophene and benzene subunits to produce **8** and **9**, respectively. Due to the more readily available cross-coupling partners, this method has been much more widely explored in our laboratory.

2.2 *Electronic and morphological characterisation*

By design, these peptides remain molecularly dissolved in aqueous solution at basic pH due to repulsion between negatively charged carboxylic acid end groups and side chains. Intermolecular self-assembly of the peptide is triggered upon protonating these groups under acidic conditions by reducing the Coulombic repulsion among the molecules and therefore encouraging interpeptide hydrogen bonding and simultaneously inducing intimate π-electron interactions between the embedded chromophores. The end result is the production of 1D nanostructures as illustrated ideally in Figure 4. A key aspect of these materials is the exciton coupling between the transition dipoles of the chromophore moieties that occur upon assembly, leading to well-characterised perturbations in the absorption and photoluminescence spectra. Therefore, absorption and photoluminescence data were acquired for all peptides to observe the extent of intermolecular exciton coupling. Figure 5 shows these data for **2–9** in both their unassembled (pH 8, dashed lines) and assembled (pH 6, solid lines) states. In general, each peptide displays a blue shift in the absorption λ_{max} and a quenching and red shift of photoluminescence upon assembly, which is indicative of cofacial H-like aggregation and/or excimeric interactions of the chromophore moieties (*33*). Although each peptide studied displayed these similar spectroscopic characteristics, slight differences are observed for individual peptides, presumably due to the differences in the identities of the chromophore subunits and their flanking peptides that collectively influence the electronic interactions within the aggregates. For instance, **4** and **5** display larger blue shifts in their absorption upon assembly (38 and 32 nm, respectively) in comparison with **6** and **7**, which show only a 15- and a 7-nm shift, respectively. Differences in the magnitudes of the observed exciton couplings among these different chromophore units can be attributed to the differences in their respective isolated excitation energies and/or the respective oscillator strengths of these transitions. Compound **7** shows a large 82-nm red shift in the photoluminescence λ_{max} upon assembly, whereas this shift is only 32–39 nm in the cases of **2**, **3**, **6**, **8** and **9**, highlighting the different contributions of excimer-like emission within the different aggregates. Relatedly, the quenching of photoluminescence upon assembly occurs with varying degrees for each peptide. The photophysics associated with these materials are quite complex and require systematic molecular variations on a per-chromophore basis to explicate in more depth (*34*). Regardless of these specific photophysical differences, it is remarkable that all peptide–π systems reported here undergo H-like self-association. Even longer oligomers embedded

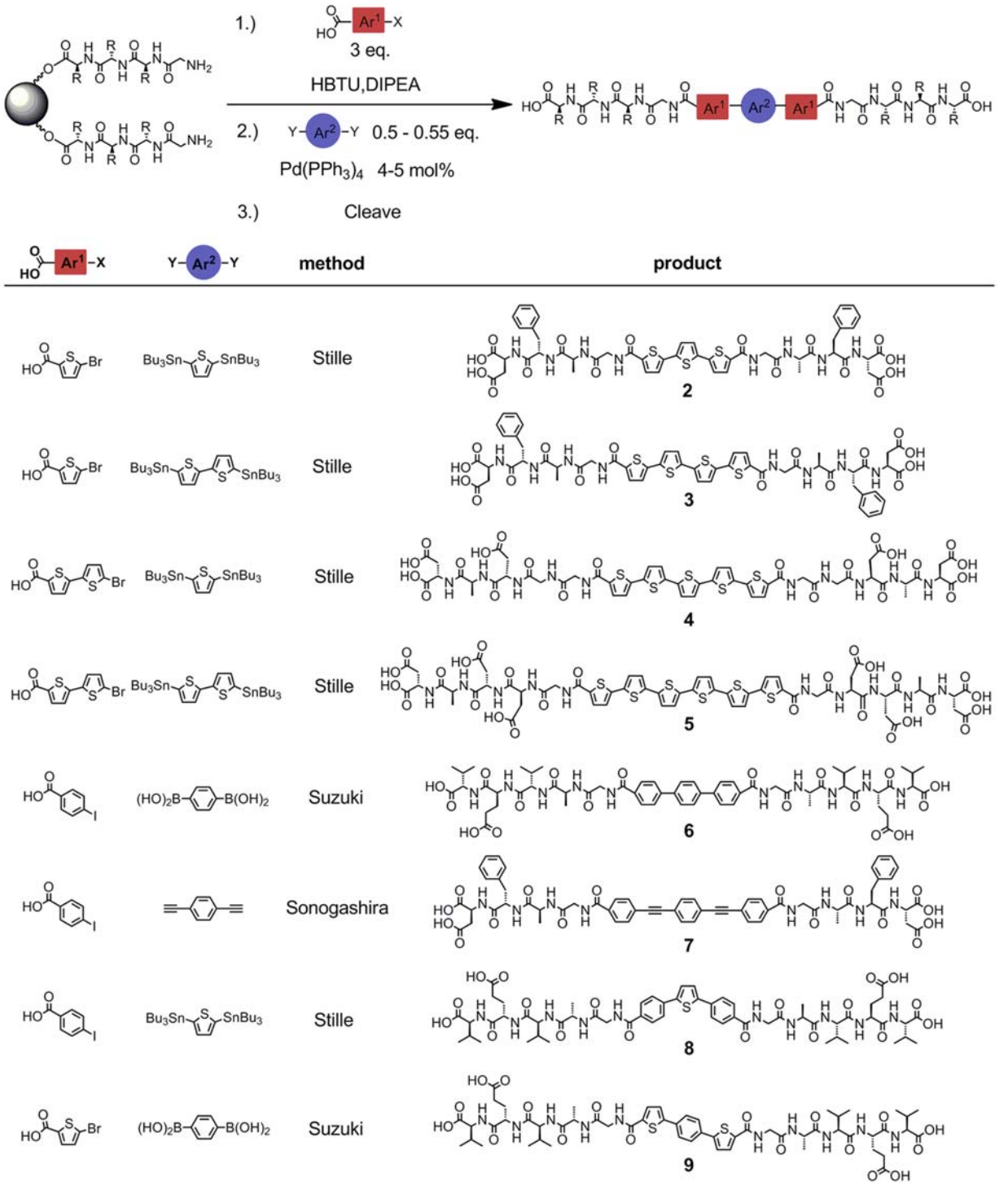

Figure 3. (Colour online) Peptides prepared from procedure 2. For Suzuki-type couplings, 8 eq. of K_2CO_3 was also included in the reaction mixture. For Sonogashira-type couplings, 10 mol% CuI and 3 ml diisopropyl amine were also included in the reaction mixture.

within **4**, **5** and **7** undergo π-stacking and 1D nanostructure formation. We are currently exploring the inter-relation of peptide sequence identity/length and chromophore identity/length to understand the driving forces behind these assemblies in more depth.

Circular dichroism (CD) can also be utilised to deduce exciton coupling between chromophore moieties, particularly those experiencing coupling in a chiral environment (*35*). CD spectra for **2–9** are shown in Figure 6. Each peptide displays no meaningful absorption above 250 nm

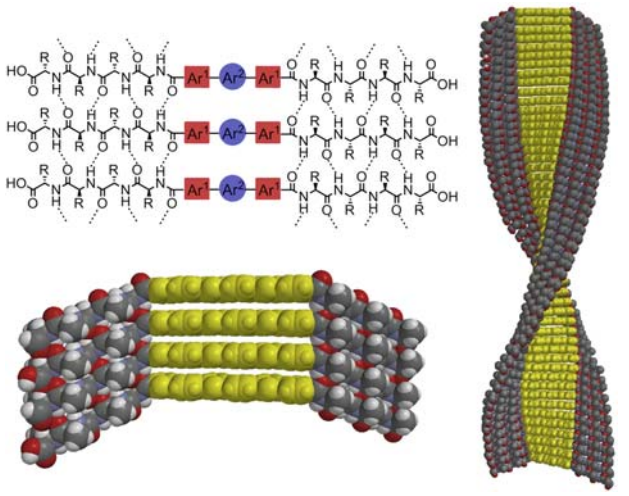

Figure 4. (Colour online) Assembly of π-conjugated peptides into 1D nanostructures.

(corresponding to the chromophore π–π* transition) when unassembled in basic solution, but upon assembly all show bisignate Cotton effects with the crossovers occurring at the λ_{max} of the respective chromophore UV–vis absorptions. This suggests that the respective chromophores interact through exciton coupling within a chiral environment, which is created by the inherently chiral assembly of the peptide scaffolds, organised into hydrogen-bonded sheet-like structures that display an overall helical twist (an idealised depiction is shown in Figure 4). Slight differences are evident between individual peptides in the amide absorption region of the CD spectra between 200 and 250 nm. Compounds **2**, **6** and **8** displayed relatively more intense signal in this region in comparison with the other studied peptides. This is possibly due to the differences in peptide assembly, brought about by variations in primary amino acid sequences. We have found that the spectral signatures associated with classical peptide secondary structures (α-helix, β-sheet, etc.) are not particularly diagnostic for these types of self-assembled materials due to their relatively disordered nature compared with standard β-sheet peptide models.

To visualise the nanostructures that are formed from the self-assembly of the chromophore-embedded peptides, transmission electron microscopy (TEM) was used. Micrographs of assembled samples of **3**, **4** and **6** are shown in Figure 7. In general, each peptide forms 1D nanostructures on the order of microns in length. Nanostructures of **3** and **4** displayed fairly uniform widths of ~6–9 nm. Molecular modelling of these peptides shows that their lengths in their most extended conformation are 4.1 and 4.9 nm, respectively. The nanostructures observed by TEM comprise individual nanostructures as well as bundles of two intertwined but well-resolved structures. Compound **6** also appears to form consistent, well-defined nanostructures with diameters of 5–7 nm, which interact with other individual structures to form bundles of various widths, some reaching nearly 40 nm. Furthermore, these extended bundled structures display a distinct right-handed helical twist.

2.3 *Investigation of electrical properties*

These two methods have allowed us to incorporate more complex π-conjugated subunits within peptide backbones than were previously possible such as the sexithiophene unit of **5**. Sexithiophene is a well-established high-performance p-channel organic semi-conductor that is

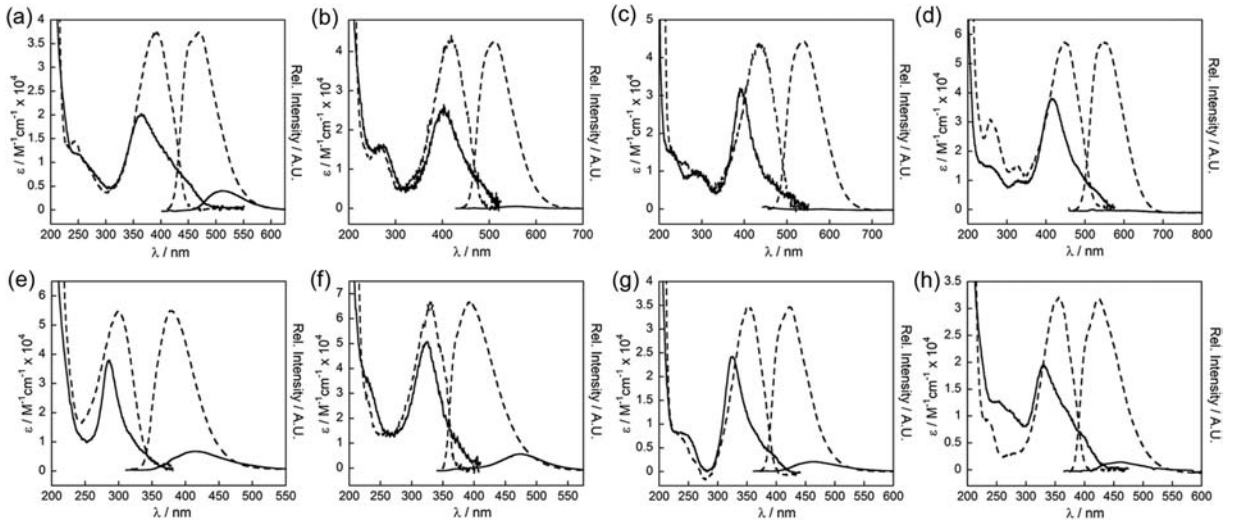

Figure 5. UV–vis and photoluminescence spectra of (a) **2**, (b) **3**, (c) **4**, (d) **5**, (e) **6**, (f) **7**, (g) **8** and (h) **9** (1.5–3.5 μM concentration) in unassembled (pH 8, dashed lines) and assembled (pH 6, solid lines) states. All spectra were taken in water.

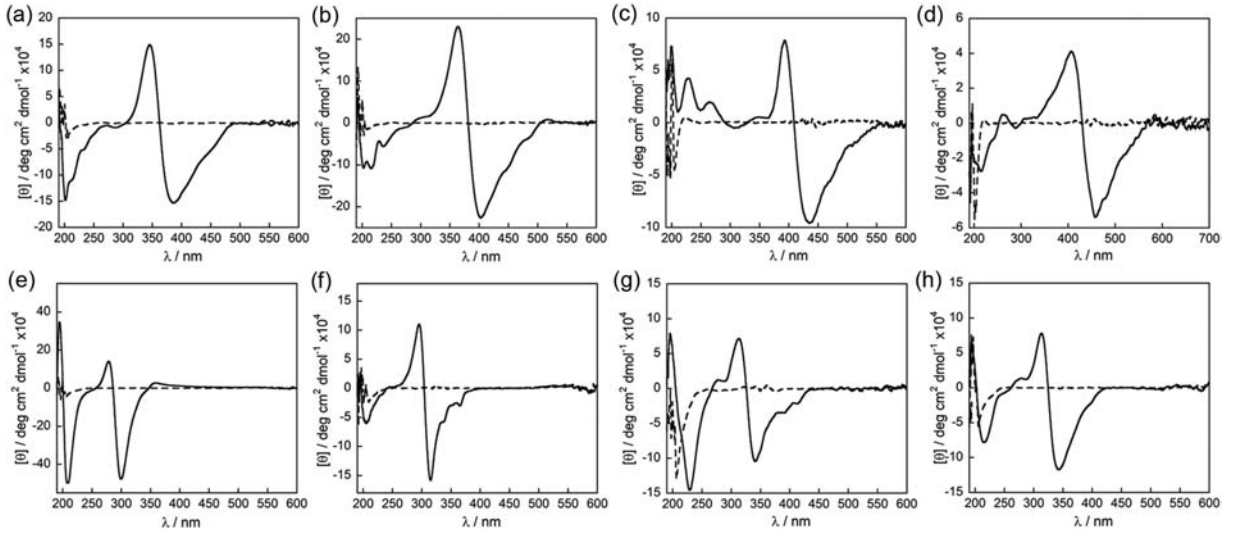

Figure 6. CD spectra of (a) **2**, (b) **3**, (c) **4**, (d) **5**, (e) **6**, (f) **7**, (g) **8** and (h) **9** (21–43 μM concentration) in unassembled (pH 8, dashed lines) and assembled (pH 6, solid lines) states. All spectra were taken in water.

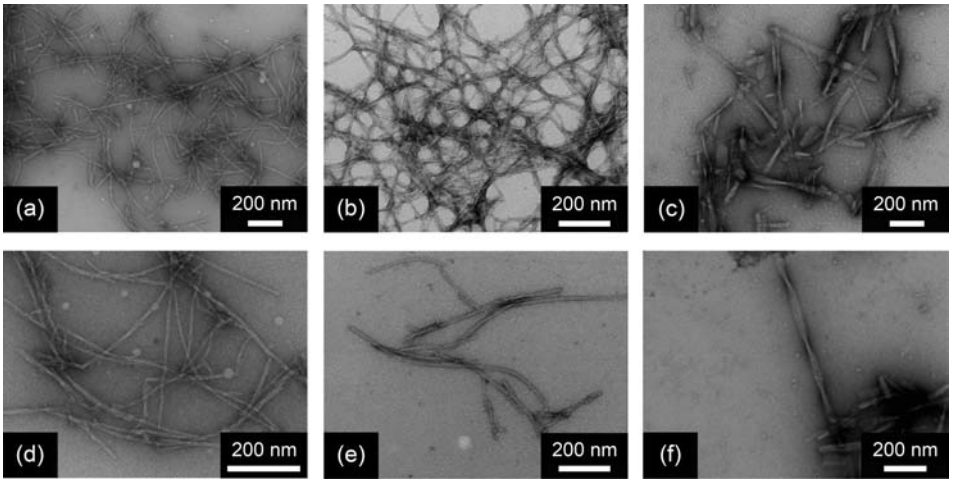

Figure 7. TEM micrographs of extended networks of (a) **3**, (b) **4** and (c) **6** and isolated nanostructures of (d) **3**, (e) **4** and (f) **6**. Samples were prepared using 1 mg/ml solutions of assembled peptide deposited on 200 mesh carbon-coated copper grids followed by staining with a 2% uranyl acetate solution.

usually included into transistor architectures via thermal evaporation. To elucidate the electrical properties that are possible with this compound in a biomimetic framework, assembled nanostructures of **5** were incorporated as the active layer of a field-effect transistor in collaboration with Prof. Howard E. Katz's group at Johns Hopkins University. A solution of **5** was dropcast on an SiO_2 substrate and then treated with concentrated HCl vapour to induce assembly. Once the sample was dry, gold source and drain electrodes were evaporated to complete the device. The hole mobility was calculated to be $3.8 \times 10^{-5}\,cm^2\,V^{-1}\,s^{-1}$ by fitting the current–voltage data to the linear equation for transistor current (*30*). Although the mobility was possibly reduced by crystal grain boundaries due to the film's polycrystalline morphology, the measurement demonstrates that these materials can transport charges through self-assembled networks. It is also important to recognise that these materials are *ca.* 70% peptidic 'insulation' that would be inherently expected to impede carrier mobility. Nevertheless, these mobilities are larger than those extracted from many other peptide-based field-effect transistor devices reported recently (*5*, *6*, *36*).

3. Conclusion

We reported two synthetic methods that utilise solid-phase palladium-catalysed cross-coupling reactions in conjunction with SPPS to construct aqueous self-assembling

peptides embedded with a variety of semi-conducting π-conjugated chromophores. In addition to easily allowing for chromophore variability and tunability while using small, soluble components that are mostly commercially available, the method also granted access to a complex sexithiophene-containing peptide, which to our knowledge is the longest self-assembling peptide–oligothiophene conjugate system to be rendered soluble in aqueous media. Each peptide displays spectroscopic features indicative of H-like aggregation upon assembly and shows 1D nanostructures in the micron-length regime under TEM. Finally, a dropcast film of **5** showed substantial hole mobility when incorporated in a field-effect transistor. Utilising this methodology for the production of these materials will aid in future bioelectronics studies.

4. Experimental

4.1 SPPS procedure

Peptides were synthesised via standard SPPS using Fmoc-protected amino acids, starting from Wang resin preloaded with the first amino acid, as described in Ref. (*30*).

4.2 General N-acylation procedure of peptides

Following completion and deprotection of the oligopeptide, the resin was treated with an aryl halide carboxylic acid (3 eq.) that was activated by HBTU (2.9 eq.) and diisopropylethylamine (10 eq.) for 2–3 h, leading to an *N*-acylated peptide capped with the desired aryl halide as previously reported (*30*).

4.3 General procedure 1 (synthesis of peptide 1)

The solid-supported peptide capped with a thienyl bromide was prepared as described earlier. The resin (0.1 mmol) was transferred to a Schlenk flask and was dried under vacuum. $Pd(PPh_3)_4$ (0.0023 g, 2 mol% relative to resin loading) was added to the reaction vessel. Fmoc-protected (5-(tributylstannyl)thiophen-2-yl) methanamine (*32*) (0.075 g, 0.12 mmol) was introduced to the resin, along with 3 ml *N,N*-Dimethylformamide (DMF). The mixture was heated to 80°C for 17 h and was agitated constantly by bubbling nitrogen through the solution. The resin was then allowed to return to room temperature and subjected to a wash cycle [3 × NMP (*N*-Methylpyrrolidone), 3 × DMF, 2 × isopropanol, 2 × water, 2× (2 × THF, 2 × isopropanol), 2 × acetonitrile, 2× diethyl ether, 2 × hexanes]. The Fmoc group was removed by treatment with a 20% piperidine solution in DMF, and standard SPPS was continued. Following the final amino acid coupling, the peptide was subjected to the same wash cycle, then a general cleavage procedure (9.5 ml of trifluoroacetic acid, 250 µl water and 250 µl of triisopropylsilane for 3 h) was performed. The peptide solution was filtered from the resin beads, washed 3 × with dichloromethane and was concentrated by evaporation under reduced pressure. The crude peptide was then precipitated from solution with 90 ml of diethyl ether and isolated through centrifugation. The resulting pellet was triturated with diethyl ether which was dissolved in ~2 ml of water and 30 µl ammonium hydroxide and lyophilised to yield crude **1** (0.055 mmol, 0.032 g, 55%). MS (MALDI) *m/z* 580.1 $(M + H)^+$ (calc. 580.2), *m/z* 602.1 $(M + Na)^+$ (calc. 602.2).

4.4 General procedure 2

A solid-supported peptide was capped with an aryl halide following the general SPPS and *N*-acylation procedures described earlier. The resin (1 eq.) was then transferred to a Schlenk flask equipped with a reflux condenser and was dried under vacuum. For Stille-type couplings, 4 mol% Pd $(PPh_3)_4$ and 0.5 eq. of the bis-stannylated aryl reagent were added to the flask along with 3–6 ml of DMF. The mixture was heated to 80°C for 16–21 h. For Suzuki-type couplings, 4 mol% $Pd(PPh_3)_4$, 8 eq. of K_2CO_3 and 0.55 eq. of 1,4-benzene diboronic acid were added to the reaction vessel with 0.5–1 ml water and 5–10 ml DMF. The mixture was heated to 80°C for 20–27 h. For Sonogashira-type couplings, 5 mol% $Pd(PPh_3)_4$, 10 mol% CuI and 0.55 eq. of 1,4-diethynyl benzene were introduced to the resin with 3 ml diisopropyl amine and 7 ml DMF. The mixture was kept at room temperature for 18 h. All reactions were agitated constantly by bubbling nitrogen through the solution throughout the course of the reaction. The resulting peptide was subjected to the general washing, cleavage and work-up procedures described earlier for **1** to yield the crude product which was then further purified by HPLC. Molecule-specific experimental stoichiometry details and characterisation data can be found in Ref. (*30*).

Acknowledgements

The authors thank Profs Raz Jelinek (Ben Gurion), Tim Hanks (Furman), Bill Pannington (Clemson) and Marc Panhuis (Wollongong) for the opportunity to present this work at the Spring 2013 MRS meeting. The authors thank Dr J. Michael McCaffery (JHU IIC) and Dr Brian Wall (Ph.D., JHU, 2013) for instrumental assistance, Dr Thomas Dawidczyk (Ph.D., JHU, 2013) and Dr Howard Katz for device measurements and Dr Stephen Diegelmann for preliminary experiments (Ph.D., JHU, 2011).

Funding

Johns Hopkins University and the Department of Energy Office of Basic Energy Sciences (DE-SC0004857, J.D.T. peptide nanomaterials) provided generous financial support.

References

(1) Schenning, A.P.H.J.; Jonkheijm, P.; Peeters, E.; Meijer, E.W. *J. Am. Chem. Soc.* **2001**, *123* (3), 409–416.
(2) Hoeben, F.J.M.; Jonkheijm, P.; Meijer, E.W.; Schenning, P.H.J. *Chem. Rev.* **2005**, *105* (4), 1491–1546.
(3) Jatsch, A.; Schillinger, E.-K.; Schmid, S.; Bauerle, P. *J. Mater. Chem.* **2010**, *20* (18), 3563–3578.
(4) Diegelmann, S.R.; Gorham, J.M.; Tovar, J.D. *J. Am. Chem. Soc.* **2008**, *130* (42), 13840–13841.
(5) Wall, B.D.; Diegelmann, S.R.; Zhang, S.; Dawidczyk, T.J.; Wilson, W.L.; Katz, H.E.; Mao, H.-Q.; Tovar, J.D. *Adv. Mater.* **2011**, *23* (43), 5009–5014.
(6) Kumar, R.J.; MacDonald, J.M.; Singh, T.M.; Waddington, L.J.; Holmes, A.B. *J. Am. Chem. Soc.* **2011**, *133* (22), 8564–8573.
(7) Schillinger, E.-K.; Mena-Osteritz, E.; Hentschel, J.; Börner, H.G.; Bäuerle, P. *Adv. Mater.* **2009**, *21* (16), 1562–1567.
(8) Shaytan, A.K.; Schillinger, E.-K.; Khalatur, P.G.; Mena-Osteritz, E.; Hentschel, J.; Börner, H.G.; Bäuerle, P.; Khokhlov, A.R. *ACS Nano* **2011**, *5* (9), 6894–6909.
(9) Stone, D.A.; Hsu, L.; Stupp, S.I. *Soft Matter* **2009**, *5*, 1990–1993.
(10) Stone, D.A.; Tayi, A.S.; Goldberger, J.E.; Palmer, L.C.; Stupp, S.I. *Chem. Commun.* **2011**, *47*, 5702–5704.
(11) Gothard, C.M.; Rao, N.A.; Nowick, J.S. *J. Am. Chem. Soc.* **2007**, *129* (23), 7272–7273.
(12) Bräse, S.; Kirchhoff, J.H.; Köbberling, J. *Tetrahedron.* **2003**, *59* (7), 885–939.
(13) Testero, S.A.; Mata, E.G. *J. Comb. Chem.* **2008**, *10* (4), 487–497.
(14) Nandy, J.P.; Prakesch, M.; Khadem, S.; Reddy, P.T.; Sharma, U.; Arya, P. *Chem. Rev.* **2009**, *109* (5), 1999–2060.
(15) Wade, J.V.; Krueger, C.A. *J. Comb. Chem.* **2003**, *5* (3), 267–272.
(16) Ruhland, T.; Svejgaard, L.; Rasmussen, L.K.; Andersen, K. *J. Comb. Chem.* **2004**, *6* (6), 934–941.
(17) Ma, Y.; Margarida, L.; Brookes, J.; Makara, G.M.; Berk, S.C. *J. Comb. Chem.* **2004**, *6* (3), 426–430.
(18) Magano, J.; Dunetz, J.R. *Chem. Rev.* **2011**, *111* (3), 2177–2250.
(19) Ohnmacht, S.A.; Brenstrum, T.; Bleicher, K.H.; McNulty, J.; Capretta, A. *Tetrahedron Lett.* **2004**, *45* (29), 5661–5663.
(20) Malenfant, P.R.L.; Fréchet, J.M.J. *Chem. Commun.* **1998**, 2657–2658.
(21) Deshpande, M.S. *Tetrahedron Lett.* **1994**, *35* (31), 5613–5614.
(22) Le Quement, S.T.; Nielsen, T.E.; Meldal, M. *J. Comb. Chem.* **2008**, *10* (3), 447–455.
(23) Doan, N.-D.; Bourgault, S.; Létourneau, M.; A. *J. Comb. Chem.* **2008**, *10* (1), 44–51.
(24) Haug, B.E.; Stensen, W.; Svendsen, J.S. *Bioorg. Med. Chem. Lett.* **2007**, *17* (8), 2361–2364.
(25) Marsault, E.; Peterson, M.L. *J. Med. Chem.* **2011**, *54* (7), 1961–2004.
(26) Conde-Frieboes, K.; Andersen, S.; Breinholt, J. *Tetrahedron Lett.* **2000**, *41* (47), 9153–9156.
(27) Blackwell, H.E.; Clemons, P.A.; Schreiber, S.L. *Org. Lett.* **2001**, *3* (8), 1185–1188.
(28) Liao, Y.; Fathi, R.; Yang, Z. *J. Comb. Chem.* **2003**, *5* (2), 79–81.
(29) Liao, Y.; Fathi, R.; Yang, Z. *Org. Lett.* **2003**, *5* (6), 909–912.
(30) Sanders, A.M.; Dawidczyk, T.J.; Katz, H.E.; Tovar, J.D. *ACS Macro Lett.* **2012**, *1* (11), 1326–1329.
(31) Vadehra, G.S.; Wall, B.D.; Diegelmann, S.R.; Tovar, J.D. *Chem. Commun.* **2010**, *46* (22), 3947–3949.
(32) Diegelmann, S.R. The Synthesis and Characterization of Self-assembling Peptides Bearing Organic-Electronic Units for the Development of Biologically Active Nanowires. Ph.D. Dissertation, The Johns Hopkins University, Baltimore, MD, 2011.
(33) Kasha, M.; Rawls, H.R.; Ashraf El-Bayoumi, M. *Pure Appl. Chem.* **1965**, *11* (3–4), 371–392.
(34) Wall, B.D.; Zacca, A.E.; Wilson, W.L.; Ferguson, A.L.; Tovar, J.D. (in press) Supramolecular Polymorphism: Tunable Electronic Interactions Within Pi-conjugated Peptide Nanostructures Dictated by Primary Amino Acid Sequence.
(35) Harada, N.; Nakanishi, K. *Acc. Chem. Res.* **1972**, *5* (8), 257–263.
(36) Sun, Y.; Jiang, L.; Schuermann, K.C.; Adriaens, W.; Zhang, L.; Boey, F.Y.C.; De Cola, L.; Brunsveld, L.; Chen, X. *Chem. Eur. J.* **2011**, *17* (17), 4746–4749.